# Bedload Adaptation Length in Gravel-bed Rivers Final Report

Project Completion Report S&T Project 3054

> David Gaeuman Yong Lai

February 24, 2014



U.S. Department of the Interior Bureau of Reclamation Peer Review Certification: This document has been peer reviewed per guidelines established by the Technical Service Center and is believed to be in accordance with the service agreement and standards of the profession.

PREPARED BY:

David Gaeuman, Ph.D. Physical Scientist Trinity River Restoration Division, Northern California Aerial Office

Yong Lai, Ph.D. Hydraulic Engineer Sedimentation and River Hydraulics Group (86-68240)

PEER REVIEWED BY:

DATE:\_\_\_\_\_

\_



U.S. Department of the Interior Bureau of Reclamation

## CONTENTS

Abstract	1
Introduction	2
Year 1 – Model Development and Numerical Simulation	4
Year 2 – Laboratory Experiments	4
Flume Configuration and Experimental Design	5
Experimental Runs	6
Discussion and Conclusions	9
References	10

## Abstract

Spatially variable channel geometry in natural rivers produces non-uniform flow and spatial gradients in the shear stress field. The travel distance required for the flow to acquire the capacity bedload concentration and attain a new equilibrium bedload transport rate upon encountering a region of higher or lower shear stress is defined as the bedload adaptation length ( $L_b$ ). Estimates of  $L_b$  are needed to account for non-equilibrium transport rates in morphodynamic models. This project addressed the need to improve methods for estimating  $L_b$  in two phases. The first phase of this study, conducted in 2012, involved the selection and development of physically-based methods for estimating  $L_b$ , and testing them, along with a selection of existing methods, by implementing them in the SRH-2D morphodynamic model. The primary result of this initial phase of investigation, which is described in an interim report for this project, is that none of the existing or newly-developed methods for estimating  $L_b$  could be shown to perform better in the numerical environment than simply assigning  $L_b$  an arbitrary constant value.

The second phase of this project involved an attempt to experimentally measure  $L_b$  in a laboratory flume. Instantaneous bedload transport rates were determined by counting passing sediment particles on digital imagery collected at variable distances downstream from a zerotransport boundary in a small flume. The flume, which is located at the University of California at Berkeley's Richmond Field Station, was operated at three bed slopes in order to assess  $L_b$  over a range of hydraulic conditions.  $L_b$  was found to be about  $30 \pm 8$  particle diameters at a relatively low transport stage (ratio of dimensionless shear stress to critical dimensionless shear stress) of 1.42, and about  $100 \pm 30$  particle diameters at a moderate transport stage of 1.74. The experiments failed to resolve  $L_b$  at higher transport stages. These results support physically-based models that cast  $L_b$  as an increasing function of excess shear stress. The Phillips and Sutherland equation is identified as the existing approach that most closely approximates the empirical measurements. It is, however, suggested that the equation could be improved by replacing a constant coefficient found in that equation with a coefficient that varies as a function of excess shear stress. It is also noted that the values of  $L_b$ found in these experiments are small relative to the resolution of the numerical mesh used in many modeling applications. In such cases, model performance may be insensitive to the choice of any arbitrary small value of  $L_b$ . Scaling  $L_b$  according to channel width or other measures of channel geometry is discouraged.

## Introduction

This investigation was conceived during the design phase of a gravel augmentation and river rehabilitation project implemented on the gravel-bedded Trinity River in California. SRH-2D, a 2-dimensional hydraulic and morphodynamic model developed at the Bureau's Technical Services Center (Lai, 2010; Lai et al. 2011), was being used to assess a design hypothesis that high-flow gravel injection would cause a gravel bar to form in a particular downstream location (Gaeuman 2013). It was observed during model calibration and validation runs using pre-project topography and historical hydrology that SRH-2D tended to incorrectly predict aggradation in existing pools. The tendency for aggradation persisted regardless of which sediment transport equations were used, and for all reasonable values of the available calibration parameters.

In addition to the sediment transport equations themselves, SRH-2D contains one additional parameter that directly affects bedload transport. Virtually all numerical morphodynamic models implement sediment transport equations that predict equilibrium sediment transport rates, that is, transport rates that are fully adjusted to local hydraulic conditions. In reality, shear stresses and other hydraulic parameters are spatially variable and sediment transport rates may not be in equilibrium with the local flow conditions. SRH-2D attempts to account for non-equilibrium transport by incorporating an 'adaptation length' ( $L_b$ ) that quantifies the travel distance required for a packet of sediment to reach a new equilibrium concentration when it moves into a region of higher or lower shear stress.

 $L_b$  is implemented in SRH-2D by modifying the sediment source term ( $S_e$ ) that defines the difference between the erosion rate (E) and the deposition rate (D) at computation nodes within the numerical mesh (Greimann et al. 2008):

$$S_e = E - D = \frac{1}{L_b} (q_b - BUhC)$$
 (1)

where  $q_b$  is the capacity transport rate computed with a user-defined bedload transport function, *B* is the ratio of sediment velocity to flow velocity, *U* is the depth-average flow velocity, *h* is the flow depth, and *C* is the depth-average bedload concentration.

Various model calibration runs performed for the Trinity River design demonstrated that the value selected for  $L_b$  had a significant effect on the degree of predicted pool filling, suggesting that proper selection of this parameter might be critical for accurately modeling morphodynamic change. However, there is currently no satisfactory theory available to quantify  $L_b$  in terms of local hydraulic and sedimentological variables. The typical approach, and the approach normally used in SRH-2D, is to assume that  $L_b$  is related to the size of dominant bedforms in the stream. Use of this type of criteria can result in estimates ranging from several times the channel width or dune or bar length (Wu et al. 2004) to sand ripple lengths (Wu et al. 2000), or even to the conclusion that L is so small as to be negligible (Armanini 1992). This method for parameterizing a numerical model cannot, in general, be correct. Even if the value assigned to  $L_b$  were in some sense optimal for the reach, a constant-

valued estimate necessarily ignores what is likely to be significant spatial variability in hydraulic and sedimentological conditions through the reach.

A few formulae cast  $L_b$  in terms of the average particle step length,  $\mu_s$ , which is in turn assumed to be a function of flow strength and particle size. Yalin (1972) suggested that  $\mu_s$  is proportional to the product of dimensionless shear stress,  $\theta$ , and particle diameter, *d*:

$$\mu_s = \alpha_s \theta d \tag{2}$$

Phillips (1981) proposed a slightly refined relation in which  $\theta$  is replaced by the dimensionless shear in excess of the critical value for particle entrainment,  $\theta_c$ . As observed by Phillips and Sutherland (1989), the proportionality constant can be defined to include  $\alpha_s$ , as well as the proportionality between  $\mu_s$  and  $L_b$ , resulting in:

$$L_b = \alpha_s \left(\theta - \theta_c\right) d \tag{3}$$

Seminara et al. (2002) suggested a similar formulation based only on particle diameter:

$$L_b = 286.4d\tag{4}$$

Lai and Gaeuman (2013) suggested that, within the context of a numerical model,  $L_b$  can be implicitly incorporated into a sediment transport equation based on the direct numerical solution of expressions quantifying the entrainment rate (*E*) and deposition rate (*D*) of bedload particles. The equations used for this purpose are due to Seminara et al. (2002):

$$\frac{E}{\sqrt{(s-1)gd}} = \alpha \left(\theta - \theta_c\right)^{3/2}$$
(5a)

$$\frac{D}{\sqrt{(s-1)gd}} = \beta \left(\theta - \theta_c\right)^{1/2} \frac{hC}{d}$$
(5b)

in which s is the specific weight of the sediment, g is gravitational acceleration, and  $\alpha$  and  $\beta$  are constants with values of 0.0199 and 0.03, respectively.

In addition to direct numerical solution of the entrainment and deposition rates, Lai and Gaeuman (2013) combined equation (5) with equation (1) to derive a closed expression for  $L_b$  in which  $V_b$  is the velocity of the bedload and  $\rho$  is the density of water:

$$L_{b} = \frac{V_{b}d}{\beta\sqrt{(\theta - \theta_{c})/\rho}}$$
(6)

The newest approach to estimating  $L_b$  was proposed in the recent work of Zhang et al. (2013), who proposed the following theoretical equation:

$$L_{b} = \frac{\left(\rho_{s} - C_{M}\rho_{f}\right)V_{b}^{2}}{P\mu_{d}\left(\rho_{s} - \rho\right)g}$$
(7)

where  $\rho_s$  is the density of sediment,  $\rho_f$  is the density of sediment-laden flow, *P* is the entrainment probability,  $\mu_d$  is the coefficient of friction, and  $C_M$  is the added mass coefficient, which is assigned a value of 0.5. The reader is referred to Zhang et al (2013) for discussion of the procedures recommended for assessing the values of *P* and  $\mu_d$ . The Zhang model departs radically from all previous work in that it predicts that  $L_b$  decreases by two orders of magnitude as shear stress increases from the threshold of entrainment to a value of  $\theta/\theta_c$  of about 10.

#### Year 1 – Model Development and Numerical Simulation

One of the objectives of this project was to test the usefulness of existing and newlydeveloped methods for incorporating the effects of  $L_b$  into the numerical modeling environment by implementing them in the morphodynamic module of SRH-2D. Three models – equations (4) and (6) used in conjunction with an equilibrium bedload transport equation plus direct numerical solution of equation (5) – were inserted in the SRH-2D code and run for reach of the Trinity River where abundant data are available to quantify changes in bed topography over a 2-year period (Lai and Gaeuman 2013). The resulting topographic changes were compared with the results obtained using a constant  $L_b$  of 80 m, which is about 2.5 times the reach-averaged channel width. All other model parameters, which had been tuned to optimize the agreement between the constant-  $L_b$  output and the observed changes, were held constant. The results of those test are detailed in an interim report filed for this project (Lai and Gaeuman 2013), so are summarized only briefly here.

Simulation results obtained using equation (6) showed little difference from those obtained using the constant adaptation length. Both tended to show more erosion in riffle areas and more deposition in pools than actually occurred. Use of equation (4) resulted in the prediction of excessive deposition everywhere, including on riffles, whereas direct solution of equation (5) resulted in excessive erosion everywhere. Lai and Gaeuman (2013) point out that implementation of equation (5) can give more reasonable results if the constant  $\alpha$  is arbitrarily reduced by a factor of 10, but the magnitude of required parameter adjustment nonetheless cast doubt on the validity of these equations.

#### Year 2 – Laboratory Experiments

The second year of this project focused on experiments designed to empirically assess  $L_b$  in a laboratory flume located at the University of California at Berkeley's Richmond Field Station. The overall experimental plan was to measure instantaneous bedload transport rates at variable distances downstream from a zero-transport boundary condition to assess the distance required for transport rates to increase from zero at the boundary to the capacity rate.

## Flume Configuration and Experimental Design

The flume used for these experiments is 5 m long and 0.3 m wide, and was loaded with uniform gravel between 2.4 and 2.8 mm in diameter (geometric mean size = 2.6 mm). A lead-in section 1.7 m in length with the same sediment glued in place was used to develop uniform flow while ensuring that sediment transport rates were zero at the beginning of the test section. A test section approximately 1 m long was established, leaving about 2.3 m of flume length between the end of the test section and the tail gate. Longitudinal stationing in the flume is hence forth measured as distance downstream from the beginning of the test section in m.

The primary imaging equipment used was a Silicon Video 1281 CMOS color camera with a 12.5-mm lens. Digital images from the camera were logged to a computer running XCAP for Windows at a rate of 60 frames per second. The camera could be rigidly mounted to the flume at three locations within the test section. Its mount was configured to position the camera at a laterally oblique angle that provided a view of the flume bed through a plexiglass side wall. This configuration was chosen to avoid image distortion from surface ripples. The resulting field of view had longitudinal spans of about 0.09 m in the foreground and 0.18 m at the base of the far side wall. From upstream to downstream, the camera mounting positions centered the field of view at stations 0.1, 0.34, and 0.73. Spatial variability in transport was quantified by counting grains passing transects defined by a 0.01-m rectangular grid superimposed on images of the flume bed. Passing grains were counted at a total of five transect lines oriented perpendicular to the flume axis. Three of those transects, at stations 0.06, 0.1, and 0.15, were defined within the view at the upstream camera position. One transect was defined at the center of the field of view at each of the remaining two camera positions. A fourth camera position and sixth transect was initially established at station 1.2, but this location proved to be within the zone influenced by non-uniform hydraulic conditions at the tail gate for some runs and so was abandoned.

All experimental runs were initiated by screeing the flume bed flat and raising the flume with a hydraulic jack near its downstream end to set a bed slope of 0.0045. A steady water flow of  $Q = 0.01 \text{ m}^3$ /s was then established throughout the flume. After some initial movements of unstable grains on the bed surface, the flume substrate quickly reached a state that appeared to be near the threshold of entrainment but with no active transport. The flow depth was measured with transparent rulers taped to the plexiglass wall of the flume, mean flow velocity (*U*) was determined as *Q* divided by the cross-sectional flow area, and bed shear stress was computed using the second approximation of Guo and Julien (2005). The values for depth, *U*, and  $\theta$  associated with this initial flume slope were found to be 0.065 m, 0.51 m/s, and 0.0436, respectively.

Once steady flow and a stable bed were well established in the flume, the valve on the hydraulic jack was opened so as to smoothly lower the downstream end of the flume to rest on wooden blocks as much as 2.5 cm lower than the initial jack height. In this manner, the slope of the flume could be rapidly increased to one of three final values -0.0067, 0.0085, or 0.01 - in less than 0.5 s. However, the hydraulic adjustments that follow any slope change takes longer, so preliminary experiments were conducted to quantify the duration of that adjustment period. These consisted of first establishing steady flow conditions at the initial

flume slope, and then increasing slope to each of the final values while using several handheld digital video devices to simultaneously record the time series of depth changes at five ruler locations along the length of the flume. These data support a quantitative analysis of the spatial and temporal changes in hydraulic conditions during the adjustment period.

The main experimental runs consist of nine sets of three runs each, for a total of 27 runs. Each set corresponds to a different combination of flume slope and camera position, with each combination being replicated in triplicate. Equilibrium hydraulic parameters associated with each flume slope are listed in Table 1, including transport stage,  $T = \theta/\theta_c$ , which serves as an index of bedload transport intensity. Here, *T* is computed with  $\theta_c = 0.0436$ , due to the fact that the flume substrate was observed to be close to the threshold of entrainment at the initial flume slope of 0.0045.

The main runs proceeded by establishing steady flow conditions at the initial slope and starting to log digital imagery before increasing flume slope as described above. The time of the slope increase was flagged by briefly obstructing the camera lens. Subsequent image acquisition continued for 30 s or more, until the operators were confident that sediment transport rates had stabilized to local equilibrium rates throughout the flume.

Runs	Slope	Depth (m)	U (m/s)	θ	Т	Camera Station
1-3	0.0067	0.061	0.54	0.062	1.42	0.01
4-6	0.0067	0.061	0.54	0.062	1.42	0.34
7-9	0.0067	0.061	0.54	0.062	1.42	0.73
10-12	0.0084	0.058	0.57	0.076	1.74	0.01
13-15	0.0084	0.058	0.57	0.076	1.74	0.34
16-18	0.0084	0.058	0.57	0.076	1.74	0.73
19-21	0.01	0.055	0.60	0.087	1.99	0.01
22-24	0.01	0.055	0.60	0.087	1.99	0.34
25-27	0.01	0.055	0.60	0.087	1.99	0.73

Table 1: Final equilibrium hydraulic parameters and camera logging station for the main experimental flume runs. U = mean flow velocity and T = transport stage. Water discharge = 0.01 m<sup>3</sup>/s for all runs.

## Experimental Results

Time series of depth changes observed at adjacent stations where digital video was recorded during the preliminary flume runs were used to construct time series of water surface slopes in the intervening flume segments. Those slopes, together with the corresponding time series of mean depths and velocities in the segments yielded estimates for the time-varying shear stresses. These data showed that dis-equilibrium hydraulic conditions persisted in the flume for up to 11 s following the change in flume slope (Figure 1). Consequently, particle transport rates observed in runs 1 through 27 cannot be representative of equilibrium conditions during the first 10 s after the slope adjustment. Particle counts obtained during the first 10 s of the high and low slope runs were therefore excluded from further analysis. Counts obtained during the first 11 s of the intermediate slope runs were excluded.

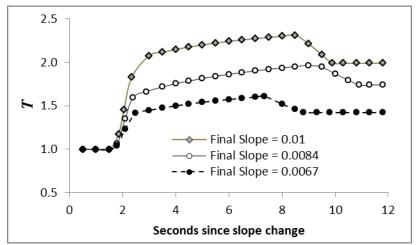


Figure 1: Time evolution of transport stage following slope adjustment in the most upstream (stations 0.03 and 0.57) of four flume segments.

Data reduction for the main experimental runs consisted of manually counting grains passing transect lines superimposed on the computer screen while scrolling through the time series of digital images. Cumulative counts were tallied as a function of elapsed time for each replicate run within the sets, and then summed to yield a total cumulative count for the set as a whole. Grain counts were obtained at transect stations 0.1, 0.34, and 0.73 for all runs. Initial review of the results showed that additional spatial resolution would be useful, so an additional transect was added at station 0.06 for the low-slope run and an additional transect was added at station 0.15 for the medium- and high-slope runs. Both of these added transect were within the field of view of the upstream camera location.

Comparisons between replicate counts at the same transect and slope and for the same elapsed time provide a rough indication of the random variability inherent in the results, whereas the summed totals constitute a larger sample and therefore give a more accurate assessment of the true transport rate. It was found that the standard deviation for replicates ranged from as little as 7% to as much as 60% of the mean, with an average of 31%. The largest percentages were associated with the low-slope runs, which averaged 49% across all transects counted.

Cumulative particle counts that graph as straight lines when plotted against elapsed time can be interpreted as representing an equilibrium transport rate. Differences between the slopes of the lines (m) corresponding to different locations in the flume therefore represent spatial differences in the transport field. Figure 2a compares the total cumulative counts at different transects for the runs conducted the lowest flume slope. Transport rates at the low slope were small (3-4 particles per s) and therefore were subject to considerable stochastic variability. The data nonetheless plot along irregular but generally linear trends that show little difference in m from one transect to another. Although the differences are small relative to the stochastic variability, it is of interest that the smallest value of m (2.90) belongs to the most upstream transect (station 0.06). The remaining three lines are approximately co-linear with m equal to about 3.7 or more. These observations suggest that the bedload transport rate is essentially fully adapted to the capacity conditions by station 0.1, or even by station 0.06. In other words,  $L_b$  is less than 0.1 m when T = 1.42.

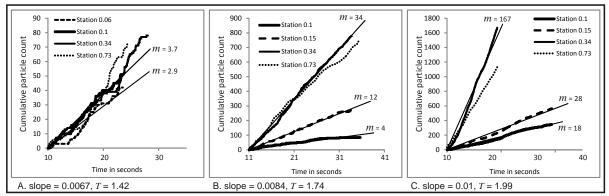


Figure 2: Total cumulative particle counts versus elapsed time for a) low-slope runs, b) medium-slope runs, c) high-slope runs.

In contrast to the low-slope data, total cumulative particle counts for the medium-slope case show a significant increase in *m* with increasing downstream distance. The value of *m* at station 0.15 is nearly three times *m* at station 0.01 and approximately a third of *m* at station 0.34 (Figure 2b). The value of *m* at station 0.73 is approximately equal to *m* at station 0.34, suggesting that transport is at the capacity rate at station 0.34. Together, these results imply that  $L_b \leq 0.34$  m and significantly larger than 0.15 when T = 1.74. Given the large difference between the values of *m* at stations 0.15 and 0.34, it is likely that the true value of  $L_b$  is considerably larger than 0.15 m. For purposes of later discussion, an arbitrary lower limit to  $L_b$  of 0.2 m is assumed.

Results for the high-slope case are more ambiguous. Again, substantial increases in *m* are evident with increasing downstream distance (Figure 2c), but there is no data to suggest where the capacity transport rate may have been reached. The difficulty is due to evidence that the downstream portion of the test section was influenced by backwater conditions during the high-slope runs. Preliminary test runs clearly showed that backwater extended upstream from the tail gate to at least station 1.2 when the flume was operated at the maximum slope. Although backwater conditions were not obvious farther upstream, the value of *m* found for the high-slope runs at station 0.73 is more than 30% smaller than *m* at station 0.34. Although it is possible that this difference reflects stochastic variability realized at two locations with equal transport rates, its proximity to a backwater zone casts doubt on whether the capacity transport rate for uniform flow was attained anywhere in the flume. Thus there can be little confidence in any upper or lower limit assigned to  $L_b$  for these runs, other than the rather trivial result that  $L_b$  for T = 1.99 is probably equal to or greater than  $L_b$  for T = 1.74.

#### **Discussion and Conclusions**

When expressed in terms of sediment particle size, the results obtained in these experiments imply that  $L_b$  is between 23 and 38 particle diameters in length when T = 1.42 and between 77 and 131 diameters when T = 1.74. Insufficient data is available to rigorously compare these results with the predictions of equations (5) or (6), but a qualitative comparison with equation (7) and quantitative comparisons with equations (3) and (4) are possible.

These flume results are clearly inconsistent with the relations proposed by Zhang et al. (2013), as their model predicts decreasing  $L_b$  with increasing transport intensity. The present results also depart markedly from equation (4) suggested by Seminara et al. (2002), in which  $L_b/d$  takes a value that is about 2 to 12 times larger than the range observed in this study, and more importantly, is constant with respect to *T*. At the most basic level, the results of this study demonstrate that  $L_b$  increases with transport intensity, at least for transport stages near the threshold of entrainment. However, the data do not preclude the possibility that  $L_b$  could attain a constant value with respect to *T*, as suggested by equation (4), at high transport intensities.

Equation (3) more closely approximates the results reported here. In their discussion of that equation, Phillips and Sutherland (1989) suggested values for the proportionality constant  $\alpha_s$  of 4000 to 9000. Using these values and  $\theta_c = 0.0436$ , equation (3) predicts values of  $L_b/d$  ranging from 74 to 166 particle diameters for T = 1.42 and from 130 to 292 diameters for T = 1.74. Thus, the range of equation (3) exceeds the range estimated from the flume experiments by a factor of 2 when T = 1.42, but equation (3) just overlaps the experimental results when T = 1.74. Inverting equation (3) and substituting in the flume-determined values of  $L_b$  suggests a range for  $\alpha_s$  of 1250 to 2100 for T = 1.42 and of 2370 to 4040 for T = 1.74. The apparent dependency of  $\alpha_s$  on T suggests modifying equation (3) to:

$$L_b = \alpha(T) \left(\theta - \theta_c\right) d \tag{8}$$

where  $\alpha(T)$  is an increasing function of excess shear stress. The form of  $\alpha(T)$  cannot be determined from two data points available at present, but equation (8) could serve as a starting point for additional investigation of this topic.

The results reported above have several implications for accommodating  $L_b$  into the numerical modeling environment. Perhaps first among them, is that the flume results indicate that  $L_b$  is short compared to the scales at which most numerical models are implemented, at least for the transport intensities typical of coarse-grained streams. For example, a typical numerical element in a 2-dimensional mesh used in models of the Trinity River might span a longitudinal distance of 6 m or more. Assuming the grain size of interest is 50-mm coarse gravel and the *T* is 1.74,  $L_b$  is likely less than 6.5 m. In such a case, the effect on equation (1) integrated over the element length would be minimal and any choice of relatively small  $L_b$  would perform similarly. In essence, the model may be too coarse to resolve the scales at which  $L_b$  affects sediment transport. However,  $L_b$  may become significant if mesh resolution is increased, suggesting that consideration of mesh size is an important factor in choosing a scale for  $L_b$  (Rahuel et al. 1989).

For applications requiring the use of a spatially variable  $L_b$ , an approach similar the one presented by Phillips and Sutherland (1989) is recommended. The simplest approach would be to implement equation (3) with  $\alpha_s$  being treated as a calibration parameter. Alternatively,  $\alpha_s$  could be replaced with an assumed form for the function  $\alpha(T)$ . For example, the two data points available from this study could yield  $\alpha(T) = 4790T - 5130$ , which may serve better than use of a constant  $\alpha_s$ .

Finally, some comment on scaling  $L_b$  according to the dimensions of morphologic elements in the channel is needed. Equations similar to (3) are conceptually related to the step lengths of bedload particles. Particle displacements in rivers are also sometimes discussed in terms of step lengths, but these steps are not equivalent to the steps that presumably contribute to determining  $L_b$ . Particle displacements in rivers include movements at a variety of scales. Displacements can be measured over the course of a flood, a run-off season, or even multiple years. These kinds of displacements may be composed of multiple shorter excursions separated by periods in which the particle is motionless for arbitrarily long periods, sometimes as a result of burial in the substrate (Hassan and Church 1994). Their relationship to morphologic features such as bars and pool-riffle sequences has been discussed by numerous authors (Hassan and Church 1992; Hassan et al. 1992; Pyrce and Ashmore 2003). This scale of movement is intertwined with variations in the channel geometry, such that particles traversing a morphologic step experience different hydraulic conditions along the way. As the morphologic and hydraulic variability that contributes to particle behavior at this scale can be incorporated into the numerical mesh, there is relatively little need to represent it with an adaptation parameter. Instead, it is appropriate to reserve  $L_b$  for representing the essentially stochastic aspects of particle entrainment and displacement that operate at the submorphologic scale.

The results of this study suggest the incorrect estimates of  $L_b$  may have little to do with the observed tendency for numerical models to over-predict aggradation in pools. This performance issue is more likely due to other factors, such as inadequate representation of turbulence and secondary flow or inaccuracies in estimates of shear stress at the bed.

## References

- Armanini, A. and G. Di Silvio, 1988, A one-dimensional model for the transport of a sediment mixture in non-equilibrium conditions, *Journal of Hydraulic Research*, 26(3):275-292.
- Gaeuman, D., 2013. High-flow gravel injection for constructing designed in-channel features. *River Research and Applications*. doi:10.1002/rra.2662.
- Greimann, B., Y. Lai and J. Huang, 2008, Two-dimensional total sediment load model equations, *Journal of Hydraulic Engineering*, 134(8):1142-1146.

- Guo, J. and P.Y. Julien. 2005. Shear stress in smooth rectangular open-channel flows, *Journal of Hydraulic Engineering*, 131(1):30-37.
- Hassan, M.A. and M. Church. 1992. The movement of individual grains on the streambed. In *Dynamics of Gravel-bed Rivers*, P. Billi, R.D. Hey, C.R. Thorne, and P. Tacconi, eds. Wiley, 159-175.
- Hassan, M.A. and M. Church. 1994. Vertical mixing of coarse particles in gravel bed rivers: A kinematic model. *Water Resources Research* 30(4):1173-1185.
- Hassan, M.A., M. Church and P.J. Ashworth. 1992. Virtual rate and mean distance of travel of individual clasts in gravel-bed channels. *Earth Surface Processes and Landforms* 17:617-627.
- Lai, Y.G. 2010. Two-Dimensional Depth-Averaged Flow Modeling with an Unstructured Hybrid Mesh. *Journal of Hydraulic Engineering* 136(1), 12-23.
- Lai, Y.G., Greimann, B.P. and Wu, K. 2011. Soft Bedrock Erosion Modeling with a Two-Dimensional Depth-Averaged Model. *Journal of Hydraulic Engineering* 137(8): 804-814.
- Lai, Y.G. and D. Gaeuman. 2013. Bedload adaptation length for modeling bed evolution in gravel-bed rivers (Interim Report), U.S. Bureau of Reclamation, Technical Services Center Report No. SRH-2013-15, 41 pp.
- Phillips, B.C. 1981. *Sediment routing in alluvial streams*, M.Eng.Sc. Dissertation, University of Melbourne, Australia, 470 pp.
- Phillips, B.C. and A.J. Sutherland. 1989. Spatial lag effects in bed load sediment transport, *Journal of Hydraulic Research*, 27(1):115-133.
- Pyrce, R.S. and P.E. Ashmore. 2003. The relation between particle path length distributions and channel morphology in gravel-bed streams: a synthesis. *Geomorphology* 56:167-187.
- Rahuel, G.T., F.M. Holly, J.P. Chollet, P.J. Belleudy, and G. Yang. 1989. Modeling of riverbed evolution for bedload sediment mixtures, *Journal of Hydraulic Engineering* 115(11):1521-1542.
- Seminara, G., L. Solari, and G. Parker, 2002, Bed load at low Shields stress on arbitrarily sloping beds: Failure of the Bagnold hypothesis, *Water Resources Research*, 38(11), 1249, doi:10.1029/2001WR000681.
- Wu, W., W. Rodi, and T. Wenka, 2000, 3D numerical modeling of flow and sediment transport in open channels, *Journal of Hydraulic Engineering*, 126(1):4-15.

- Wu, W., 2004, Depth-averaged two-dimensional numerical modeling of unsteady flow and nonuniform sediment transport in open channels, *Journal of Hydraulic Engineering*, 130(1): 1013–1024.
- Yalin, M.S. 1972. Mechanics of sediment transport, Pergamon Press, New York, 298 pp.
- Zhang, S., J.G. Duan and T.S. Strelkoff. 2013. Grain-scale nonequilibrium sedimenttransport model for unsteady flow, *Journal of Hydraulic Engineering*, 139(1):22-36.